

# Structural Relaxation Processes in Polyethylene Glycol/CCl<sub>4</sub> Solutions by Brillouin Scattering

M. Pochylski,<sup>\*,†</sup> F. Aliotta,<sup>\*,‡</sup> Z. Błaszczak,<sup>†</sup> and J. Gapiński<sup>†</sup>

*Division of Optics, Department of Physics, Adam Mickiewicz University, Poland, and  
Istituto per I Processi Chimico Fisici del CNR, sezione di Messina, Italy*

*Received: October 26, 2004; In Final Form: December 16, 2004*

We present results of a Brillouin scattering experiment on solutions of poly(ethylene glycol) of mean molecular mass 600 g/mol (PEG600) in CCl<sub>4</sub>. The relaxation process detected has been assigned to conformational rearrangements of the polymeric chains, triggered by reorientation of the side groups. The concentration dependencies of the hypersound velocity and normalized absorption are compared against the indications from several models proposed in the literature. The concentration evolution of the system is described in terms of two distinct regimes. At high polymer content, the system is dominated by the structure of the dense polymer, where polymer–polymer interactions, together with excluded volume effects, induce the existence of a preferred local arrangement resulting in a narrow distribution of the relaxation times, with the average value of the relaxation time following a simple Arrhenius temperature dependence. As the concentration decreases, the original structure of the hydrogen bonded polymer network is destroyed, and a number of different local configuration coexist, giving rise to a wider distribution of relaxation times or to a multiple relaxation. At low concentrations, the experimental data are well fitted assuming a Vogel–Fulker–Tammon behavior for the average relaxation time. In addition, the observed deviation from the ideal behavior for the refractive index and the density suggests that CCl<sub>4</sub> does not behave as an inert solvent, and due to polarization effects, it can develop local hetero-associated structures via electrostatic interaction with the O–H end groups of the polymeric chains. The hypothesis has been successfully tested by fitting the concentration behavior of the hypersonic velocity to a recent three-component model, suitable to describe the concentration dependence of sound velocity in moderately interacting fluids. The indication of the model furnishes a very high value for the association constant of the PEG600, confirming the literature indication that, in polymeric systems capable of developing long liner aggregates via hydrogen bonding interaction, the Brillouin probe is insensitive to the true length of the polymeric chains. The Brillouin scattering experiment just sees an effective hydrogen bonded aggregate that is huge relative to the length of the single polymeric chain and becomes sensitive only to the density fluctuations of the local segmental motions.

## 1. Introduction

Poly(ethylene glycol) (PEG) is a synthetic polymer of great significance in industry and, in particular, in biomedicine. As indicated by its structural formula, OH–(CH<sub>2</sub>CH<sub>2</sub>–O)<sub>n</sub>H (*n* = degree of polymerization), the hydrophobic ethylene units are arranged together with hydrophilic oxygen atoms along the polymer chain which is responsible for the unique characteristics of the compound. One of the consequences of PEG molecular structure is the existence of several hydrogen bonding sites (each of them is connected with the unshared outer electronic pair of ether oxygen) which allow formation of inter- as well as intramolecular hydrogen bonds.<sup>1</sup> The existence of the active sites along the polymer chain is also responsible for its high solubility in water as well as in a wide range of organic solvents.

Earlier studies of PEG (or POE) mixtures have been mainly restricted to dilute solutions in various solvents,<sup>2–7</sup> the interest being mainly focused on conformational changes and aggregations of POE chains driven by polymer–solvent interactions. For biomedical application reasons, most of the works have

concerned PEG aqueous solutions. On the other hand, several industrial applications require the knowledge of the behavior of POE chains in highly concentrated solutions. In particular, some interest has been directed to the investigation of the mechanisms responsible for the high ionic conductivity observed in systems obtained by dissolving a small amount of salt in a POE matrix.<sup>8</sup> Many desirable properties are undoubtedly related to dynamical properties of polymer chains, which can change in the presence of a small amount of solvent molecules. Also in the presence of a noninteracting or moderately interacting solvent, the changes in the local density of the polymeric network influence, in the first place, the process of fast localized motions of structural units of the polymeric chain which, in bulk PEG, proceeds on the picosecond time scale.<sup>9–11</sup> This fact makes the Brillouin spectroscopy a widely used technique in binary solution studies,<sup>12–17</sup> one of the more suitable tools for the investigation of the relaxation dynamics taking place in our viscoelastic polymeric melts and to study the effects of the interchain bond density on the distribution function of the relaxation times. The shape of this function is related to different processes taking place in the system and to different distributions of local topologies established via hydrogen bonding. To separate the effects of the local density of the hydrogen bond

<sup>\*</sup> Corresponding authors. E-mail: aliotta@me.cnr.it (F.A.); pochyl@amu.edu.pl (M.P.).

<sup>†</sup> Adam Mickiewicz University.

<sup>‡</sup> Istituto per I Processi Chimico Fisici del CNR.

network from those driven by solvent–polymer interactions, it becomes of importance to study polymer solutions in non-interacting solvents. Carbon tetrachloride, due to its nonpolar character, appears as the best candidate for this purpose, and a number of experimental studies have been recently performed on solutions of several hydrogen bonding systems in  $\text{CCl}_4$ .<sup>12–14</sup> Soon it has become evident that the assumption of the absence of any interactions between  $\text{CCl}_4$  and a polar solute can be taken just as a rough approximation.<sup>13,14</sup> In fact, carbon tetrachloride, also being intrinsically an apolar molecule, is highly polarizable. The numerical results from *ab initio* molecular orbital simulations in the acetone/ $\text{CCl}_4$  cluster<sup>18–19</sup> suggested that the atomic quadrupolar effect is important for electrostatic interactions around covalently bonded atoms on the third and higher rows in the periodic table. It has been recently suggested that, in mixtures of  $\text{CCl}_4$  with polar molecules, some molecular configurations can be established giving rise to hetero-structures characterized by an interaction energy probably higher than that between  $\text{CCl}_4$  molecules.<sup>13,14</sup> On this basis, we can hypothesize that hetero-aggregates can be established, via electrostatic interaction, between the polarized  $\text{CCl}_4$  molecules and the polar groups of the polymer chains. In this paper, we present the results of a Brillouin scattering experiment on binary solutions of poly(ethylene glycol) of average molecular weight 600 g/mol (PEG600) in carbon tetrachloride. The experimental data obtained are analyzed in terms of different literature models. The outcomes are compared in order to make evident the approximations involved in each model and different limits of each theoretical description. The possible role played by hetero-aggregation is also discussed.

## 2. Experimental Section, Handling of Data and Results

PEG of mean molecular mass 600 g/mol and carbon tetrachloride ( $\text{CCl}_4$ ) were obtained from Fluka Chemie GmbH and POCh Gliwice-Poland, respectively, and have been used without any further purification procedure. Solutions were prepared as equidistant weight fractions, mixing the polymer with double-distilled  $\text{CCl}_4$  and covering the whole concentration range, from pure PEG600 to pure  $\text{CCl}_4$ .

The Brillouin scattering experiment has been carried out by means of a Sandercock-type (3+3)-pass Tandem Fabry–Perot interferometer, working at a free spectral range of 15 GHz. The working finesse, estimated by the line-width of the elastic line, was about 80. The linearly polarized line ( $\lambda = 532$  nm) of a Coherent DPSS 532 laser, working at a mean power of about 100 mW, was used as the exciting irradiation. In each measurement, the VV component of scattered light has been collected in a 90° geometry.

The samples were contained in a quartz cell which was placed in a specially built thermostatic holder, whose temperature was controlled within an accuracy of  $\pm 0.1$  K. In Figure 1, we present, as an example, the Brillouin spectra, obtained at  $T = 323$  K, for some selected solutions at different values of the monomer molar fraction,  $x'$ , which is defined as

$$x' = \frac{n_{\text{OE}}}{n_{\text{OE}} + n_{\text{solv}}}$$

$n_{\text{OE}}$  being the mean number of oxyethylene units of PEG chains in solution and  $n_{\text{solv}}$  the number of the solvent molecules.

The refractive index of each solution was measured by a standard Pulfrich refractometer at four different wavelengths and in the temperature range 288–325 K. The values of

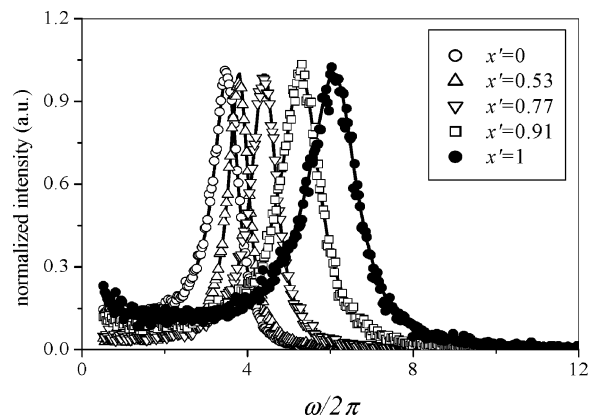


**Figure 1.** Normalized Stokes side of VV spectra for selected solutions measured at  $T = 323$  K. Solid lines are the fitting results with eq 1. Concentrations are expressed in monomer molar fraction.

refractive index at  $\lambda = 532$  nm were obtained by fitting the Cauchy equation to the experimental data. The density values in the 288–325 K temperature range were obtained using an Anton Paar DMA38 density meter. The values of the index of refraction and density at higher temperatures were estimated by extrapolation of the experimental data, under assumption of linear temperature dependencies for these parameters. The experimental concentration dependencies of the density and of the refractive index are reported in Figure 2.

The spectra recorded were fitted according to the usual expression<sup>20,21</sup>

$$I_{\text{VV}}(\omega) = \frac{A_{\text{R}}\Gamma_{\text{R}}}{\omega^2 + \Gamma_{\text{R}}^2} + A_{\text{B}} \left[ \frac{\Gamma_{\text{B}}}{[\omega - \sqrt{\omega_{\text{B}}^2 - \Gamma_{\text{B}}^2}]^2 + \Gamma_{\text{B}}^2} + \frac{\Gamma_{\text{B}}}{[\omega + \sqrt{\omega_{\text{B}}^2 - \Gamma_{\text{B}}^2}]^2 + \Gamma_{\text{B}}^2} \right] + \frac{A_{\text{B}}\Gamma_{\text{B}}}{\sqrt{\omega_{\text{B}}^2 - \Gamma_{\text{B}}^2}} \left[ \frac{\omega + \sqrt{\omega_{\text{B}}^2 - \Gamma_{\text{B}}^2}}{[\omega + \sqrt{\omega_{\text{B}}^2 - \Gamma_{\text{B}}^2}]^2 + \Gamma_{\text{B}}^2} - \frac{\omega - \sqrt{\omega_{\text{B}}^2 - \Gamma_{\text{B}}^2}}{[\omega - \sqrt{\omega_{\text{B}}^2 - \Gamma_{\text{B}}^2}]^2 + \Gamma_{\text{B}}^2} \right] \quad (1)$$

The first term in the above equation describes the central Rayleigh line of width  $\Gamma_{\text{R}}$  and intensity  $A_{\text{R}}$ . The next two terms describe the symmetric contributions to the Brillouin scattering profile ( $A_{\text{B}}$ ,  $\Gamma_{\text{B}}$ , and  $\omega_{\text{B}}$  are the intensity, the half width at half-maximum (HWHM), and the Brillouin line shift, respectively), whereas the last two terms represent the asymmetric contributions, arising from the first moment preservation selection rule. The values of the parameters  $\Gamma_{\text{B}}$  and  $\omega_{\text{B}}$ , obtained by fitting eq 1 to experimental spectra, are reported in the upper half of Figure 3 at different values of the monomer molar fraction,  $x'$ .

The values of the fitting parameters, together with those of the measured refractive indices and densities, were used to calculate the values of the hypersound velocity,  $v_{\text{B}}$ , and of the normalized sound absorption,  $\alpha/f^2$ , according to the relations<sup>20,21</sup>

$$v_{\text{B}} = \omega_{\text{B}}/q \quad (2)$$

$$\alpha/f^2 = 2\pi\Gamma_{\text{B}}/(v_{\text{B}}\omega_{\text{B}}^2) \quad (3)$$

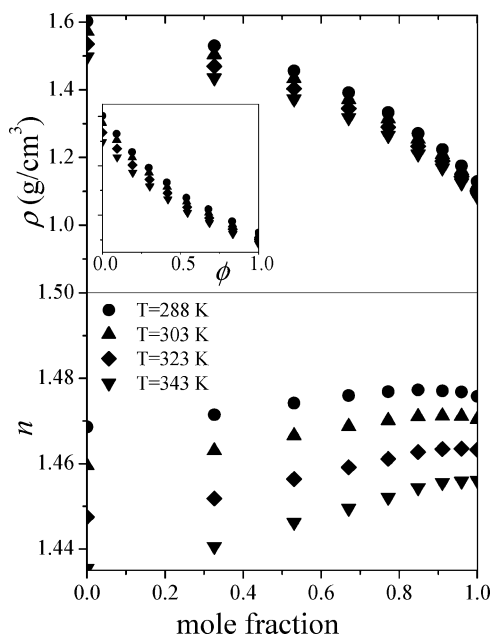


**Figure 2.** Density,  $\rho$ , and refractive index,  $n$ , experimental values, reported as a function of the PEG600 monomer mole fraction. The inset reports the behavior of the density of the PEG600/CCl<sub>4</sub> mixtures as a function of PEG600 volume fraction.

where  $q = (4\pi n/\lambda_0) \sin(\theta/2)$  is the amplitude of the exchanged wave-vector,  $\lambda_0$  is the incident wavelength, and  $\theta$  is the scattering angle.

### 3. Discussion

The temperature dependencies of the frequency shifts and of the HWHMs of the Brillouin lines observed at the different concentrations clearly show that some relaxation process is taking place on a time scale of the order of picoseconds, which can be associated with the polymeric component of our mixtures. In fact, the HWHM of the Brillouin profile for pure PEG600 exhibits a maximum at about  $T = 300$  K, whereas the plot of the Brillouin shift vs temperature deviates from the linear behavior, suggesting the existence of a inflection point at about the same temperature at which HWHM reaches it maximum

value. In highly concentrated solutions of PEG600 in carbon tetrachloride, we can observe an analogous result: the relaxation frequency moves toward higher values (the maximum of  $\Gamma_B$  moves toward lower temperatures) as the polymer concentration decreases. For pure solvent, no relaxation is observed since both frequencies and  $\Gamma_B$  values behave linearly with  $T$  in agreement with the usual increase of the compressibility with temperature, trivially resulting from the lowering of the density on heating. In highly diluted mixtures, it becomes difficult to distinguish between contributions from the polymer and the solvent, but also in these systems, the experimental data suggest some relaxation processes taking place at much lower temperatures. However, the limited ranges of the explored frequencies and temperatures do not allow observation of the maximum of  $\Gamma_B$ ; as a consequence, in our discussion of the results obtained for diluted mixtures, we will restrict our analysis within a qualitative approach. The same suggestion of a relaxation process connected with the polymeric component of the mixture comes from an inspection of the temperature dependence of the hypersonic velocity and normalized absorption. The maximum of the normalized absorption appears shifted to temperatures higher with respect to that observed from the corresponding  $\Gamma_B$  values; however, this could not be surprising if one takes into account that  $\nu_B$  and  $\alpha/f^2$  values are affected by the temperature dependence of the refractive index,  $n$ .

The observation of a relaxation phenomenon is not an unusual result for moderately viscous molten polymers or for polymeric solutions,<sup>10,22–25</sup> and it has been often assigned to the conformational rearrangements of the polymeric chains, triggered by the reorientation of the side groups. To analyze and identify the observed relaxation process, we have to find a theoretical formalism capable of describing the experimental temperature dependencies of the acoustic parameters. The linear viscoelastic theory can be a suitable approach, at least if the viscosity of the system does not assume too high values.<sup>19,22</sup> In this framework, the dynamical structure factor,  $S(\mathbf{q}, \omega)$ , describing the Brillouin doublet scattering profile is related to the Fourier transform of the density–density correlation function and depends on both the real and imaginary part of the longitudinal relaxation modulus  $M^*(\omega)$ . Generally, a relaxation process takes place with an appropriate relaxation time distribution function,

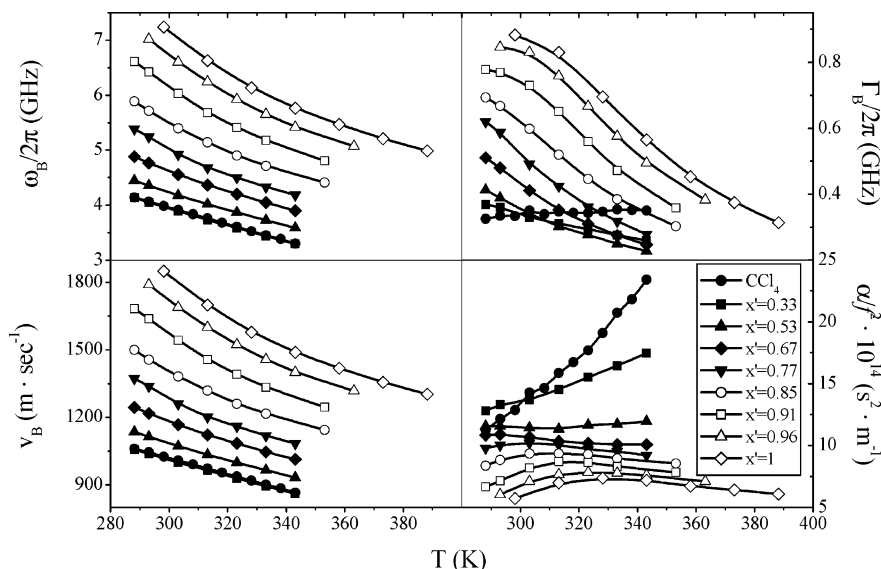


**Figure 3.** Top: temperature behaviors of the experimental Brillouin frequencies,  $\omega_B$ , and half line-widths,  $\Gamma_B$ , reported at different PEG600 contents. Bottom: temperature behavior of the hypersonic velocity and absorption data, as obtained by the fitting parameters,  $\omega_B$  and  $\Gamma_B$ , in agreement with eq 2. Continuous lines are a guide for the eye.

$g(\tau)$ , and we can write<sup>26</sup>

$$M^* = M' + iM'' = M_0 - (M_\infty - M_0) \int_0^\infty g(\tau) \frac{i\omega\tau}{1 + i\omega\tau} d\tau \quad (4)$$

The adoption of eq 4 in order to write the correct hydrodynamic expression for  $S(\mathbf{q}, \omega)$  implies that a number of difficulties concerning the knowledge of the frequency dependencies of the real and imaginary parts of  $M^*(\omega)$  in the GHz region and of the shape of the relaxation time distribution function need to be overcome.

A simplified model can be adopted under the assumption that the relaxation strength of the longitudinal modulus is small compared with the average value of  $M(\omega)$  (or, equivalently, that the strength of the hypersonic frequency relaxation is small compared with the average value of  $\omega_B$ ).<sup>9,22</sup> A further simplifying assumption follows from the experimental observation that, in a number of viscous fluids, the relaxation time distribution function turns out to be suitably described in terms of a single relaxation time<sup>25,27–29</sup> (or by a distribution of relaxation times so narrow to become indistinguishable from a single relaxation time over the limited frequency range accessible in a Brillouin scattering experiment). Under such a hypothesis, it becomes possible to obtain information about the relaxation process by fitting the experimental data for  $\omega_B$  and  $\Gamma_B$  with the equations<sup>27</sup>

$$\omega_B = \omega_s \left[ 1 + \frac{(R-1)\omega_s^2 \tau^2}{2(1 + \omega_s^2 \tau^2)} \right] \quad (5)$$

$$\Gamma_B = \frac{(R-1)\omega_s^2 \tau^2}{2(1 + \omega_s^2 \tau^2)} + \Gamma_b$$

where  $R$  is the relaxation strength of the longitudinal modulus,  $\omega_s$  describes the high-temperature behavior of  $\omega_B(T)$ , and the term  $\Gamma_b$  contains the contributions from thermal diffusion and vibration-translational coupling; the value of this latter parameter, in pure polymer, was found to be nearly equal to zero.<sup>10</sup> In fitting our experimental data for pure PEG600 with eq 5, the  $\omega_s(T)$  dependence has been obtained by extrapolating the high temperature  $\omega_B(T)$  values toward the low-frequency literature values from an ultrasound experiment.<sup>30,31</sup> Analysis of the data from the mixtures was restricted to the concentration values as low as  $x' = 0.67$ , a concentration range where, as above stressed, we are allowed to assume that the relaxation process takes place within the experimentally explored  $(\omega, T)$  region. In the fitting procedure of the experimental data from polymeric solutions, we have assumed that

$$\omega_s(T) = \omega_s^a + T\omega_s^b \quad (6)$$

$$R(T) = R^a + TR^b$$

The values of  $\omega_s^a$  and  $R^a$  have been adopted as the fitting parameters, whereas the values of slopes  $\omega_s^b$  and  $R^b$  have been fixed at the same value obtained for pure PEG600.

For the temperature dependence of the single relaxation time, a simple Arrhenius law has been assumed

$$\tau = \tau_0 \exp\left(\frac{E}{R_g T}\right) \quad (7)$$

with  $E$  being the activation energy of the relevant relaxation process and  $R_g$  the universal gas constant. The results of the simultaneous fits of eq 5 to the experimentally measured

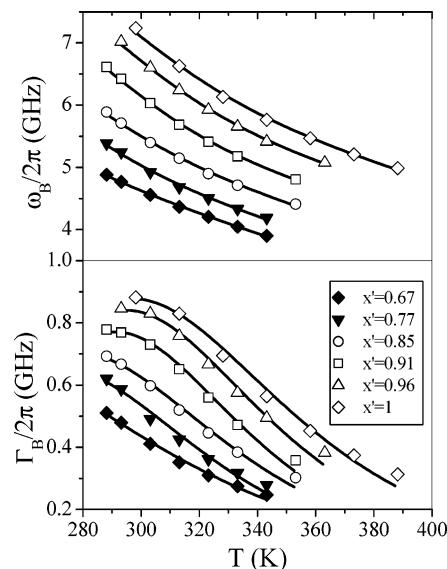


**Figure 4.** Temperature behaviors of the experimental Brillouin frequencies and half line-widths for samples at  $x' \geq 0.67$ . Continuous lines represent the result of the fitting with eq 5.

**TABLE 1: Fitting Parameters Obtained Using Eq 2 with  $\omega_s^b = -0.0134$ ,  $R^b = -0.0015$ ;  $\Gamma_b = 0$**

$x'$	$\omega_s^a$ [GHz]	$R^a$	$\tau_0 \times 10^{-13}$ [s]	$E$ [kJ/mol]
1	10.09	2.03	1.11	14.03
0.96	9.82	2.03	0.56	15.67
0.91	9.43	2.01	0.40	16.40
0.85	9.03	1.96	1.67	12.50
0.77	8.68	1.94	1.46	12.68
0.67	8.41	1.93	11.77	6.98

frequency shifts and line-widths of the Brillouin lines are presented in Figure 4, whereas the values of the parameters obtained have been collected in Table 1.

The agreement between the experimental values and the adopted model seems to confirm that the approach introduced by Wang and co-workers<sup>10,22</sup> can be suitable also for our mixtures. Also the obtained values for  $\tau_0$  and the activation energy turns out of the same order of magnitude as those observed in similar systems.<sup>10,22</sup> However, the model appears to underestimate the high-temperature values of the normalized absorption. In addition, the values of the parameters obtained for the mixture at  $x' = 0.67$  differ from the values obtained for more concentrated solutions. Probably, at this concentration, the maximum of the HWHM of the Brillouin line has already moved to a temperature lower than those experimentally explored (and the flex in the  $\omega_B$  data also has); as a consequence, the uncertainties of the values of the fitting parameters become too large. In addition, as the polymer concentration decreases, the contribution from the solvent becomes not-negligible. Despite the apparent ability of the adopted model to fit the experimental data, it becomes clear that the agreement between theory and experiment is only qualitative, as it can be deduced by an inspection of Figure 5.

In this figure, the relaxation times, calculated from the condition  $\omega\tau \sim 1$  (open squares), are presented together with the relaxation times obtained through the fitting procedure (open triangles) at the temperatures of the absorption maxima. It can be observed that, although the two sets of data show the same qualitative dependence on concentration and temperature, the relaxation times obtained by the Wang model are underestimated by about a factor of 2 with respect to the values deduced from the position of the maximum in the  $\alpha/f^2$  curves.



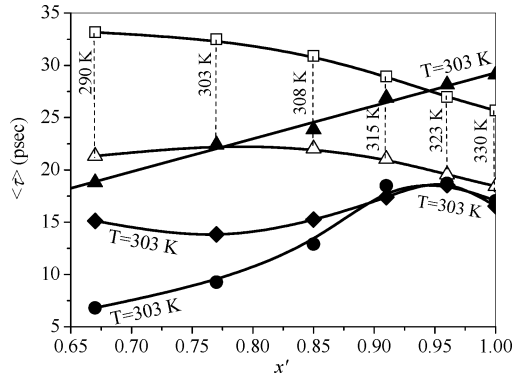


**Figure 5.** Concentration dependence of the average relaxation time, as deduced by different analytical procedures. Open squares:  $\langle\tau\rangle$  as estimated from the position of the maximum in the hypersonic absorption. Open triangles: estimates of eq 5 at the temperatures of the maxima in the  $\alpha/f^2$  plots. Filled triangles: estimates of eq 5 at  $T = 303$  K. Filled diamonds: outcomes of eq 9 under assumption of a simple arrhenian behavior for  $\langle\tau\rangle$ . Filled circles: outcomes of eq 9 under assumption of a VFT behavior for  $\langle\tau\rangle$ .

We can advance two different hypotheses in order to rationalize the observed discrepancy. On one hand, we have to take into account that the Wang model describes just the behavior of the experimental shifts and HWHMs of the Brillouin lines, fully disregarding any dependence from the refractive index values, directly involved in the determination of the hypersonic velocities and normalized absorptions through the value of the exchanged wave vector. Taking into consideration the concentration and temperature dependencies of the refractive index, the frequency position of the maximum of HWHM with respect to that of the normalized absorption becomes different. Besides, the above discrepancy could be an indication of a distribution of relaxation times (asymmetrically distributed) instead of a single relaxation time: under such conditions the outcome of the Wang model fitting procedure furnishes the value of the average relaxation time that can differ from that deduced from the position of the maximum of  $\alpha/f^2$ . In Figure 5, the concentration dependence of the relaxation time obtained at a fixed temperature,  $T = 303$  K (filled triangles), is also reported.

The first attempt to find a more suitable model can be pursued by coming back to eq 4 and trying to use it to fit the hypersonic velocity and absorption data. In fact, the real and imaginary parts of the complex modulus,  $M^*$ , are related to the adiabatic sound velocity and to the acoustic losses through the relations<sup>26</sup>

$$\begin{aligned} M' &= \rho v_B^2 \\ M'' &= \frac{\Gamma_B}{\omega_B} M' \end{aligned} \quad (8)$$

where  $\rho$  represents the macroscopic density. Under the assumption of a single relaxation process, from eq 8, taking into account the hyper-acoustic normalized absorption definition, we obtain

$$\begin{aligned} v_B^2(\omega, T) &= v_0^2(T) + (v_\infty^2(T) - v_0^2(T)) \frac{\omega^2 \tau^2(T)}{1 + \omega^2 \tau^2(T)} \\ \frac{\alpha}{f^2}(\omega, T) &= \frac{2\pi^2}{v_B^3(T)} (v_\infty^2(T) - v_0^2(T)) \frac{\tau^2(T)}{1 + \omega^2 \tau^2(T)} + C \end{aligned} \quad (9)$$

where  $v_0$  and  $v_\infty$  are the low and high-frequency limit values of the sound velocity,  $\tau$  is the structural relaxation time, and  $C$  is

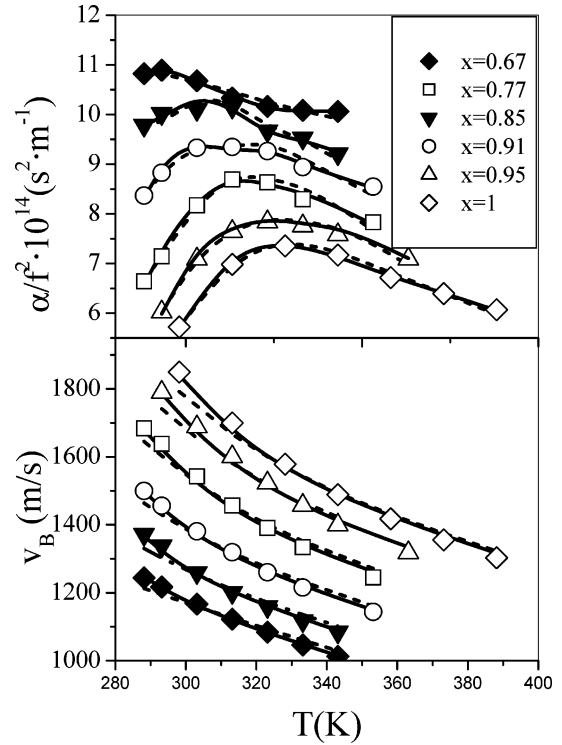


**Figure 6.** Comparison between the results of fitting the experimental data with eq 5, under the assumption of a single arrhenian relaxation time (dashed lines) and of a Vogel–Fulcher–Tamman law (continuous lines).

**TABLE 2: Results of the Fitting Procedure with Eq 9, under Assumption of a Simple Arrhenian Behavior of the Relaxation Time**

$x'$	$\tau_0 \times 10^{-13}$ [s]	$E$ [kJ/mol]
1	0.22	16.7
0.96	0.22	16.5
0.91	0.22	18.4
0.85	0.22	16.0
0.77	0.22	15.4
0.67	0.21	13.7

a constant taking into account all the nonrelaxing high-frequency contributions.

Equation 9 should furnish the same results as eq 6, if the validity conditions of the Wang model are fulfilled. In fitting our data with eq 9, the low-frequency velocity data for pure PEG600 have been taken from ref 30, the slopes of  $v_0$  data have been fixed at the same value of pure PEG600, whereas the constant term was taken as an adjustable parameter, adopting a procedure similar to the one employed in modeling the frequency data with the Wang equations. Also in this case, we assumed a simple Arrhenian behavior for the relaxation time. In Figure 6, the results of the fitting procedure are reported as dashed lines.

In Table 2, the obtained values for  $\tau_0$  and the activation energy are reported. Although the activation energies are very close to the results of the Wang model, the values of  $\tau_0$  are systematically lower. Also the relaxation times at  $T = 303$  K (filled rhombuses in Figure 5) are lower than those suggested by the Wang model. The concentration dependence of the relaxation time looks quite different from that deduced by the Wang model. The relaxation time turns out to increase with the concentration up to  $x' < 0.9$  then the plot flattens.

The behavior suggested by the adoption of the model described by eq 9 shows a close similarity to the concentration

dependence of the refractive index. This observation would suggest that eq 9 can be a better model for fitting our data than eq 5. In effect, the two sets of equations reduce to the same model until we are allowed to assume a small relaxation strength and until any concentration dependence of the bulk macroscopic properties of the system can be regarded as negligible or, at least, following an ideal behavior. In our case, this last assumption is not fulfilled, as we can deduce from the concentration dependencies of the refractive index and density (see Figure 2). In this respect, different concentration behaviors obtained for the relaxation times from the two models are not surprising, if one takes into account that the dependence of the fitted data on the refractive index is an immediate result of the dependence of the calculated sound velocity on the exchanged wave vector.

Although eq 9 could be considered as a more suitable model for fitting our data, the same discrepancies between the theory and experimental results are observed. In particular, the model does not seem to reproduce well the experimental velocity data at low-temperature values, near the relaxation frequency. This can be taken as a further suggestion that the calculated relaxation time has to be interpreted just as the average value of a distribution of relaxation times.

In effect, the assumption of a structural relaxation process described by a single relaxation time could be a too crude approximation in our case. The local structure of molten PEG600, in fact, is dominated by hydrogen bonding interactions among neighboring chains. As for almost any hydrogen bonded network,<sup>32</sup> we are allowed to expect that there is a distribution of local arrangements to which a distribution of local minima in the potential energy hypersurface corresponds. In addition, the energy barrier between adjacent minima is of the order of the thermal energy (in order to obtain a change of the local configuration we have only to wait for the breaking and reforming process of a few hydrogen bonds). The situation becomes also more complicated in the mixtures with CCl<sub>4</sub>. In fact, assuming that carbon tetrachloride acts as an inert solvent (and we will show in the sequel that this can be taken just as a very rough approximation), the dilution will change the kinetic equilibrium between the breaking and reforming process of hydrogen bonding, directly depending on the rate of collisions between active sites. As a consequence, a change in this kinetic equilibrium will be reflected not only in a change of the values of the average relaxation time but also in a change of the shape of the distribution function of the relaxation times. To fix the nature of the relaxation process that we observe, we have to take into account that the universal picture of relaxing dynamics in polymers assumes the existence of two distinct regimes: the high-temperature regime where the system is dominated by a single relaxation process and the low-temperature regime where two distinct processes are observed. The low-frequency process is related to micro-Brownian diffusive motions driving the glass transition of the system, whereas the fast process is described in terms of side-group or end-group rotations.<sup>22–25,33,34</sup> The low frequency process is too slow to contribute to the Brillouin doublet, arising due to the adiabatic pressure fluctuation time correlation function, and only gives rise to a not propagating local contribution to the depolarized Rayleigh scattering, related to the constant pressure density fluctuation (or entropy fluctuations) correlation function.<sup>22–24</sup> On this basis, we are confident that the observed process can be related to a local fast conformational structural relaxation of the polymeric chain that splits from the single high-temperature process when a crossover temperature,  $T_C$ , is approached.

**TABLE 3: Results of the Fitting Procedure with Eq 9, under Assumption of a VFT Behavior of the Average Relaxation Time**

$x'$	$T_0$ [K]	$\tau_0 \times 10^{-12}$ [s]	$D$
1	208.6	1.22	1.18
0.96	214	1.66	1.01
0.91	214.3	2.00	0.90
0.85	217.7	1.98	0.80
0.77	227.5	2.28	0.60
0.67	237.4	2.89	0.46

In agreement with the above consideration, we tried a new fit of our data with eq 9, where the temperature dependence of the average relaxation time was assumed to follow a Vogel–Fulcher–Tamman relation

$$\tau = \tau_0 \exp\left(\frac{DT_0}{T - T_0}\right) \quad (10)$$

instead of the simple Arrhenius law.

This assumption implies the existence of multiple distribution of relaxation times.  $T_0$  represents the temperature at which the average value of the relaxation time diverges (a structural arrest takes place that can be related to the glass transition).

The coefficient  $D$  contains both an enthalpic and an entropic contribution, in agreement with the idea that the structural relaxation time is governed by the state of the system disorder (configurational entropy) being at the same time a function of the height of the energy barrier that the cooperatively rearranging groups have to pass over.<sup>35–37</sup>

The results of the fitting procedures are shown, as continuous lines, in Figure 6. The improvement is clearly evident in the low-temperature behavior of the velocity data. Also the fits of the absorption data are of a better quality. Table 3 reports the values of the fitting parameters, whereas the values of the average relaxation time at  $T = 303$  K are given in Figure 5 (filled circles). As follows from these data, at concentrations higher than  $x' = 0.9$ , the results obtained under the assumption of a simple arrhenian relaxation time are almost coincident with those obtained assuming the Vogel–Fulcher–Tamman behavior. This observation would suggest that, at high density of the dispersed phase, the polymer–polymer interactions together with the excluded volume effects drive the establishment of a preferred local arrangement resulting in a narrow distribution of relaxation times.

This interpretation is supported by a good agreement between the results obtained by fitting the data obtained for pure PEG600 and the solution at  $x' = 0.96$  with the different models. Under dilution, the breaking and reforming processes of the local hydrogen-bonded network allow the formation of a wider distribution of local topologies to which a wider distribution of relaxation times corresponds. As a consequence, the temperature dependence of the average relaxation time diverges from the simple Arrhenian behavior as lower concentration systems are taken into account.

The fact that our systems seem to be characterized by a distribution of relaxation times, which are related to the existence of some local configurations, mainly promoted by entropic effects and stabilized by low energy bindings, would suggest for describing our solutions as weakly interacting liquid mixtures and to adopt a literature model able to furnish a value of the conditional association constant starting from acoustic data.<sup>38,39</sup> According to this model, the molar equilibrium association

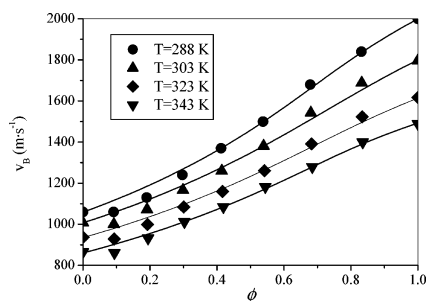


**Figure 7.** Volume fraction dependencies of the hypersound velocity in PEG600/CCl<sub>4</sub> solution at different temperatures. Continuous lines represent the results of fitting with eq 12.

constant  $K_{As}$  can be defined as

$$K_{As} = \frac{c_{As}}{(c_P - c_{As})(c_C - c_{As})} \quad (11)$$

where  $c_C$  and  $c_P$  are the initial molar concentrations of carbon tetrachloride and PEG600, respectively, and  $c_{As}$  is the molar concentration of the hypothetical (hetero-) associated species.

In adopting the model<sup>38</sup> to fit the sound velocity data,  $v_h$ , for our mixtures, we assumed the additivity of the time of transmission of the acoustic signal with the volume fractions  $\phi_P$ ,  $\phi_C$ , and  $\phi_{As}$  of the components<sup>40</sup>

$$v_h = \frac{v_P v_C v_{As}}{\phi_P v_C v_{As} + \phi_C v_P v_{As} + \phi_{As} v_C v_P} \quad (12)$$

where  $v_P$ ,  $v_C$ , and  $v_{As}$  are the sound velocities in pure PEG600, carbon tetrachloride, and the hetero-associated species, respectively. In adopting eqs 11 and 12, we have to know the densities of the three constituents. The densities  $\rho_C$  and  $\rho_M$  of the pure components are known, but we have to advance some assumptions about the value of  $\rho_{As}$ . As a rough estimate, we adopted the average value of the pure compounds, as in ref 38; fortunately, as it has been generally observed,<sup>14,39</sup> the outcomes of the model are only slightly influenced by this last value.

Our fitting procedure furnished a value of 0.15 for the association constant, almost independent of temperature, whereas the hypersound velocity in the hypothetical hetero-structure was estimated as linearly dependent on temperature, ranging from 1858 m/s at 15 °C to 1403 m/s at 70 °C. The estimate for  $K_{As}$  is probably too high (a systematic investigation of different systems indicates typical values of the order of 0.01<sup>39</sup>); however, we have to notice that such a value can be largely affected by self-association of PEG600 that we are not explicitly taking into account in eq 11. In this respect, the results from a recent Brillouin scattering experiment on poly(propylene glycol) (PPG)<sup>41</sup> confirm earlier suggestions<sup>42</sup> that low molecular weight PPG behaves as a longer chain molecule. This finding can explain why the obtained value of  $K_{As}$  could be overestimated. The fitting results are reported, as continuous lines, in Figure 7 at four different temperatures.

#### 4. Concluding Remarks

Our experimental data clearly show that in molten PEG600 a relaxation process, which proceeds in the GHz frequency range, is observed. Consistently with literature results on polymeric fluids,<sup>9,23</sup> we assigned this process to a high frequency conformational rearrangement of the polymeric chains driving the reptational dynamics (taking place on a time scale much longer than that accessible in a Brillouin scattering experiment)

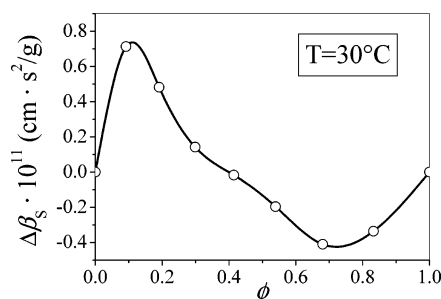


**Figure 8.** Excess adiabatic compressibility at  $T = 30$  °C, reported as a function of the PEG volume fraction.

and becoming faster when our polymer is dissolved in carbon tetrachloride.

This observation agrees with the general idea that these conformational rearrangements are triggered by the local reorientations of the side groups, which becomes more probable in diluted systems.

In our case, the situation can be complicated by the occurrence that the observed relaxation dynamics is not only to be related to polymer–polymer interactions but also to some nonnegligible solvent–polymer interactions taking place via electrostatic forces. On this basis, one can try to describe our solutions as mixtures of moderately interacting liquids in terms of a three component model successfully adopted in the literature. On a qualitative level, the model seems to be able to reproduce our experimental data, but some differences between theory and experiment deserve some comments. In particular, it can be observed that the model seems able to reproduce with enough accuracy the data from mixtures at the volume fractions of the polymeric phase higher than 0.3. At lower concentrations, the results predicted by the model become overestimated. An explanation of such a result can be deduced from Figure 8. The excess value of the adiabatic compressibility  $\Delta\beta_s$ , defined as a difference between experimentally observed adiabatic compressibility ( $\beta_s = 1/\rho v_B^2$ ) and its ideal value, calculated as the volume average between the values for pure CCl<sub>4</sub> and pure PEG600 ( $\beta_{s,id} = \beta_{CCl_4} + (\beta_{PEG} - \beta_{CCl_4})\phi$ ), is shown as a function of the volume fraction  $\phi$ .

It can be seen that the volume fraction value of 0.3 marks the transition from the regime, at high polymer content, in which the excess compressibility is lower than the ideal one (negative  $\Delta\beta_s$  values) to a new regime, at low polymer concentration, where the system becomes more compressible (positive  $\Delta\beta_s$  values). We can hypothesize that when we start adding carbon tetrachloride to pure PEG600, the local structure of PEG600 is retained and that CCl<sub>4</sub>, due to polarization effects, interacts with the polymeric component strengthening its original structure. In this high concentration regime, the three component model seems to work well enough. When the number of solvent molecules added to the system overcomes the number of molecules that can be engaged in the local polymeric network, it becomes probable that some CCl<sub>4</sub> molecules are surrounded by like molecules giving rise to local configurations similar to those observed in bulky CCl<sub>4</sub>. As a consequence, the compressibility of the system will lower after dilution approaching that of the pure solvent. The observed failure of the model at low polymer content can be taken as a further confirmation of the above-described structural changes upon dilution. At low polymer concentrations, the original PEG600 connectivity is lost, a number of different local topologies coexist, and the three component model is no more able to reproduce the experimental behavior of the hypersonic velocity. This conclusion agrees well with our observation that, in diluted systems, the assumption

of a simple Arrhenius relaxation process is no more appropriate and the existence of multiple distributions of relaxation times should be taken into consideration.

## References and Notes

- (1) Smith, G. D.; Yoon, D. Y.; Jaffe, R. L.; Colby, R. H.; Krishnamoorti, R.; L. J. Fetters, L. J. *Macromolecules* **1996**, *29*, 3462.
- (2) Sengwa, R. J. *Polym. Int.* **1998**, *45*, 202.
- (3) Koziełski, M.; Muhle, M.; Błaszczak, Z. *J. Mol. Liquids* **2004**, *111*, 1.
- (4) Polverari, M.; van de Ven, T. G. M. *J. Phys. Chem.* **1996**, *100*, 13687.
- (5) Picarra, S.; Pereira, E. J. N.; Bodunov, E. N.; Martinho, J. M. G. *Macromolecules* **2002**, *35*, 6397.
- (6) Liu, K. J. *Macromolecules* **1968**, *1*, 213.
- (7) Liu, K. J.; Parsons, J. L. *Macromolecules* **1969**, *2*, 529.
- (8) Seneviratne, V.; Furneaux, J. E.; Krech, R. *Macromolecules* **2002**, *35*, 6392.
- (9) Lin, Y. H.; Wang, C. H. *J. Chem. Phys.* **1978**, *69*, 1546.
- (10) Wang, C. H.; Li, B. Y.; Rendell, R. W.; Ngai, K. L. *J. Non-Cryst. Solids* **1991**, *131*, 870.
- (11) Noudou, T.; Matsuoka, T.; Koda, S.; Nomura, H. *Jpn. J. Appl. Phys.* **1996**, *35*, 2944.
- (12) Sassi, P.; D'Elia, V.; Cataliotti, R. S. *Physica B* **2003**, *325*, 349.
- (13) Aliotta, F.; Ponterio, R.; Salvato, G.; Musso, M. *J. Phys. Chem. B* **2004**, *108*, 732.
- (14) Aliotta, F.; Musso, M.; Ponterio, R.; Saija, F.; Salvato, G. *J. Phys. Chem. B* **2004**, *108*, 12972 and references therein.
- (15) Kawase, S. *J. Phys. Soc. Jpn.* **1995**, *64*, 1785.
- (16) Kawase, S.; Maruyama, K.; Tamaki, S.; Okazaki, H. *J. Phys.: Condens. Matter* **1994**, *6*, 10237.
- (17) Matsuura, H.; Fukuhara, K. *Bull. Chem. Soc. Jpn.* **1986**, *59*, 763.
- (18) Torii, H. *Chem. Phys. Lett.* **2002**, *365*, 27.
- (19) Torii, H. *J. Chem. Phys.* **2003**, *119*, 2192.
- (20) Boon, J. P.; Yip, S. *Molecular hydrodynamics*; McGraw-Hill: New York, 1980.
- (21) Berne, B. J.; Pecora, R. *Dynamic light scattering*, Wiley-Interscience (New York, 1976).
- (22) Wang, C. H.; Fytas, G.; Zhang, J. *J. Chem. Phys.* **1985**, *82*, 3405.
- (23) Engberg, D.; Schüller, J.; Strube, B.; Sokolov, A. P.; Torell, L. M. *Polymer* **1999**, *40*, 4755.
- (24) Lehman, S. Y.; McNeil, L. E.; Albalak, R. *J. Polym. Sci.* **2000**, *38*, 2170.
- (25) Aliotta, F.; Di Marco, G.; Fontanella, M. E.; Lanza, M. *J. Phys.: Condens. Matter* **1998**, *10*, 545.
- (26) Ferry, J. D. *Viscoelastic Properties of Polymers*, 3rd ed.; Wiley: New York, 1984.
- (27) Lin, Y. H.; Wang, C. H. *J. Chem. Phys.* **1979**, *70*, 681.
- (28) Lampert, W.; Wang, C. H. *J. Chem. Phys.* **1980**, *72*, 2570.
- (29) Lampert, W.; Wang, C. H.; Fytas, G.; Dorfmueller, Th. *J. Chem. Phys.* **1982**, *76*, 2570.
- (30) Maisano, G.; Majolino, D.; Migliardo, P.; Venuto, S.; Aliotta, F.; Magazù, S. *Mol. Phys.* **1993**, *78*, 421.
- (31) Donato, I. D.; Magazu, S.; Maisano, G.; Majolino, D.; Migliardo, P.; Pollicino, A. *Mol. Phys.* **1996**, *87*, 1463.
- (32) Angell, C. A. *Hydrogen-bonded liquids*; Dore, J. C., Texeira, J., Eds.; Kluwer: Dordrecht, 1991.
- (33) Wu, L. *Phys. Rev. B* **1992**, *49*, 9906.
- (34) Murthy, S. S. N.; Sobhanadri, J.; Gangasharan, J. *J. Chem. Phys.* **1994**, *100*, 4601.
- (35) Adam, G.; Gibbs, J. H. *J. Chem. Phys.* **1965**, *43*, 139.
- (36) Gibbs, J. H. *Modern aspects of the vitreous state*; Butterworth: London, 1960.
- (37) Angell, C. A. *J. Phys. Solids* **1988**, *49*, 863.
- (38) Glinzki, J. *J. Sol. Chem.* **2001**, *31*, 59.
- (39) Glinzki, J. *J. Chem. Phys.* **2003**, *118*, 2301.
- (40) Natta, G.; Baccaredda, M. *Atti. Acad. Naz. Lincei* **1948**, *4*, 360.
- (41) Ko, J. H.; Kojima, S. *Phys. Lett. A* **2004**, *321*, 141.
- (42) Wang, C. H.; Huang, Y. Y. *J. Chem. Phys.* **1976**, *64*, 4847.